ACS OMEGA

Article

http://pubs.acs.org/journal/acsodf

Rapidly Responding pH- and Temperature-Responsive Poly (*N*-Isopropylacrylamide)-Based Microgels and Assemblies

Andrews Ahiabu and Michael J. Serpe*

Department of Chemistry, University of Alberta, Edmonton, Alberta, Canada T6G 2G2

Supporting Information

ABSTRACT: Rapidly responding stimuli-responsive materials can have a benefit in a myriad of applications, for example, sensing and biosensing, actuation, and in drug delivery systems. Thermo- and pH-responsive materials have been among the most widely studied, and can be triggered at physiologically relevant temperatures and pH. Here, we have used a "homologous series" of acids based on the acrylic acid (AAc) backbone and incorporated them into *N*-isopropylacrylamide (NIPAm)-based microgels. Specifically, the acids used were AAc, methacrylic acid (MAAc), ethylacrylic acid (EAAc), and butylacrylic acid (BAAc), which have pK_a's in the range of 4.25−7.4. The resultant microgels were characterized by optical microscopy, and their responsivity to temperature and pH studied by dynamic light scattering. The microgels were subsequently used to generate optical devices (etalons) and their pH and temperature response was also investigated. We found that the devices composed of BAAc-modified microgels exhibit unusually fast response kinetics relative to those of the rest of the devices. We also found that the speed of the response decreased as the length of the acid pendant group decreased, with AAc-modified microgel-based devices exhibiting the slowest response kinetics. Finally, we showed that the kinetics of the device's temperature response also decreased as the length of the acid pendant group decreased, which we hypothesize is a consequence of the hydrophobicity of the acid groups, that is, increased hydrophobicity leads to faster responses. Understanding this behavior can lead to the rational design of fast responding materials for the applications mentioned above.

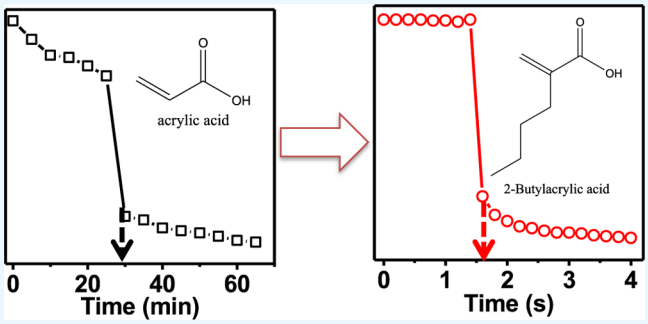

INTRODUCTION

Stimuli-responsive polymers (or simply responsive polymers) that respond to their environment by undergoing changes in their chemical and/or physical properties have been known for a number of decades. Specifically, responsive polymers have been developed that respond to changes in solution pH,[1−5] temperature,[5−10] ionic strength,[11,12] and the application of an electric field,[13] magnetic field,[14] and/or light.[6,15] Of the various stimuli-responsive polymers, those that respond to changes in temperature are the most extensively studied, and poly (*N*-isopropylacrylamide) (pNIPAm) has emerged as the most popular polymer over the past few decades.[10] Since its first discovery in 1968,[16] pNIPAm has been used for numerous applications including: sensing and biosensing,[17,18] drug delivery,[19−21] tissue engineering,[22] antifouling coatings,[23] and "smart" optical systems.[8] This is partially a result of pNIPAm's volume phase transition temperature (VPTT) of 32 °C, which is near the range of physiological relevance. Specifically, below this temperature, pNIPAm exists as a random coil (extended state), and transitions into a globular conformation (collapsed state) above 32 °C. Furthermore, pNIPAm is "hydrated" below the VPTT and "dehydrated" above the VPTT; this transition is fully reversible over many cycles.

Cross-linked polymer networks composed of pNIPAm can also be generated, and exhibit behavior similar to that of pure pNIPAm. That is, the materials (hydrogels) are swollen with water below the VPTT, and deswollen above the VPTT. Hydrogel particles (microgels) can also be synthesized, and behave similarly to hydrogels; they have also found numerous applications.[24−26] Their relative "ease" of synthesis and the ability to vary the microgel chemistry/responsivity via simple copolymerization, has made the use of microgels very attractive. For example, to make pNIPAm-based microgels pH responsive, a weak acid/base can be copolymerized into the network. A common pH-responsive monomer that is used is acrylic acid (AAc), which has a pK_a of ∼4.25. Upon copolymerizing with NIPAm, the network becomes responsive to pH due to the ionization of AAc at pH > pK_a, which causes the gel to swell as a result of charge−charge repulsion and an increase in the material's osmotic pressure.[27] The network returns to its initial state at pH < pK_a. This phenomenon has been exploited for pH sensing,[28] ion sensing, and drug delivery.[19] Other pH-responsive comonomers have been studied including MAAc,[29,30] maleic anhydride (MA),[31] vinyl acetic acid (VAA),[29] and *N*,*N*′-dimethyl aminoethyl methacrylate (DMAEMA).[32] Although these responsive materials are well known,

Received: February 2, 2017
Accepted: April 18, 2017
Published: May 3, 2017

DOI: 10.1021/acsomega.7b00103
ACS Omega 2017, 2, 1769−1777

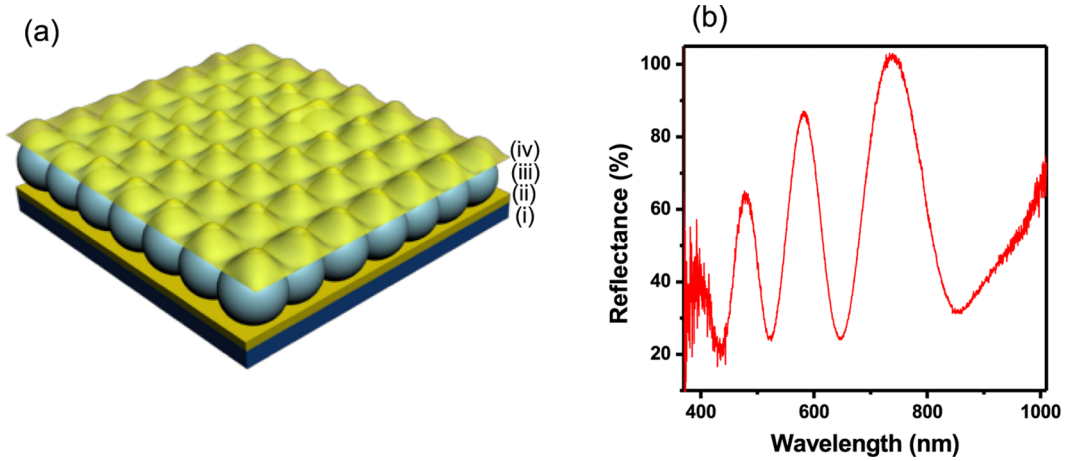

Figure 1. (a) Structure of etalon: (i) glass substrate, (ii) Cr/Au underlayer, (iii) microgel layer, (iv) Cr/Au overlayer. (b) A representative reflectance spectrum from a microgel-based etalon showing multiple peaks as a result of the order term "*m*" in eq 1.

their application has been limited by their relatively slow response time to solution pH changes. Hence, new materials with fast response times to solution pH are desired to realize new applications.

Our group is interested in fabricating pH sensors from responsive polymers composed of monomers with pK_a values covering the entire pH scale. In the process of fabricating these pH sensors, we observed that variations in the alkyl chain length of the pendant group on AAc-based comonomers shifts the pK_a toward more physiologically relevant pHs, which is similar to what was observed by Grainger et al.[33] More importantly, we observed that the speed of the response was significantly improved as the length of the pendant alkyl chain increased. As mentioned before, materials with fast response kinetics to pH changes are needed for various applications, such as: actuators for chemical valves,[34] artificial muscles,[35] and "on/off" switches for controlling chemical reactions.[36] To achieve such materials, Zhang et al.[37] reported on the fabrication of a comb-type grafted hydrogel, by grafting free pNIPAm and pDMAEMA chains onto the backbone of a cross-linked pNIPAm-*co*-pDMAEMA network. They reported a faster swelling rate and higher swelling degree (at lower pH) for the grafted hydrogels compared to that of the native cross-linked pNIPAm-*co*-pDMAEMA hydrogels. In another example, Yan et al.[38] copolymerized a polymeric surfactant, poly(2-(methacryloyl-oxy)decyl phosphate), with pNIPAm to generate gels with improved response kinetics. They observed an 88% swelling ratio within 30 min and a complete collapse within 120 min (from the swollen state) in response to temperature. This is in contrast to the 24% swelling ratio within 30 min for the unmodified pNIPAm gels. To obtain macroscopic gels with fast response to external stimuli, Richtering and co-workers[39] embedded pNIPAm-based microgels in a polyacrylamide hydrogel matrix. The embedded microgels rendered the microgel−polyacrylamide composite thermo-responsive, yielding a faster response relative to the hydrogels themselves. Several other studies have been devoted to improving the response time of pH/thermo-responsive systems using various grafting approaches.[40−42]

In this investigation, we demonstrate that the pH-dependent response kinetics could be varied by manipulating the chain length of the pendant group attached to the second carbon of AAc. Specifically, the response kinetics to solution pH changes become faster as the alkyl chain length increases. To investigate this, we synthesized a series of acid modified microgels via free radical precipitation polymerization. The weak acid monomers differed from one another by the length of their alkyl group, that is, AAc, methacrylic acid (MAAc), ethylacrylic acid (EAAc), or butylacrylic acid (BAAc). The resultant microgels were characterized by differential interference contrast (DIC) microscopy and dynamic light scattering (DLS) at various solution temperatures and pH. Similar to microgels made of AAc, the microgels composed of MAAc, EAAc, and BAAc could be ionized at solution pH above their respective pK_a of 5.5, 6.3, and 7.4.[33]

We go on to show that optical sensing devices (etalons[43]) could be constructed from these microgels and used to monitor real time solution pH. This was accomplished by constructing layered materials composed of two thin Au layers sandwiching the pNIPAm-based microgels. A schematic of the structure of the etalons can be seen in Figure 1a, and these were generated by depositing a thin layer of Au (typically 15 nm) on top of a glass substrate followed by the deposition of the microgel layer and a subsequent layer of Au on top of the deposited microgel layer. This device exhibits color, and the multipeak reflectance spectra can be seen in Figure 1b. This is due to light impinging on the device resonating in the microgel-based cavity, leading to constructive/destructive interference, which allows certain wavelengths of light to be reflected, according to eq 1

$$m\lambda = 2nd\cos\theta \quad (1)$$

where m is the order of a "reflected" peak, λ is the reflected wavelength at a given order of reflection, n is the refractive index of the dielectric medium, d is the distance between the two Au mirrors, and θ is the angle of incident light. In our experiments, θ was maintained at 0°, and with negligible change in n, and for a particular order m, we see a direct relationship between λ and d. Therefore, any stimuli that can change the etalon's d-spacing will result in a color change, which can be used for sensing applications. Although these devices exhibit optical properties that depend on temperature due to the thermo-responsive behavior of the pNIPAm-based microgels, the presence of AAc, MAAc, EAAc, and BAAc in the microgels also affects the device's color dependent on pH. That is, when the surrounding solution has a pH > pK_a, the microgel's acid groups are ionized, resulting in their swelling and a change in (d) and the wavelength of light reflected from the device, leading to a color change. We observed the response kinetics to

DOI: 10.1021/acsomega.7b00103
ACS Omega 2017, 2, 1769−1777

Scheme 1. (a) Structures of pH-Responsive Monomers Used for This Study and (b) Polymerization Scheme Used To Generate Poly(*N*-isopropylacrylamide-*co*-butylacrylic Acid) (pNIPAm-*co*-BAAc) Microgels[a]

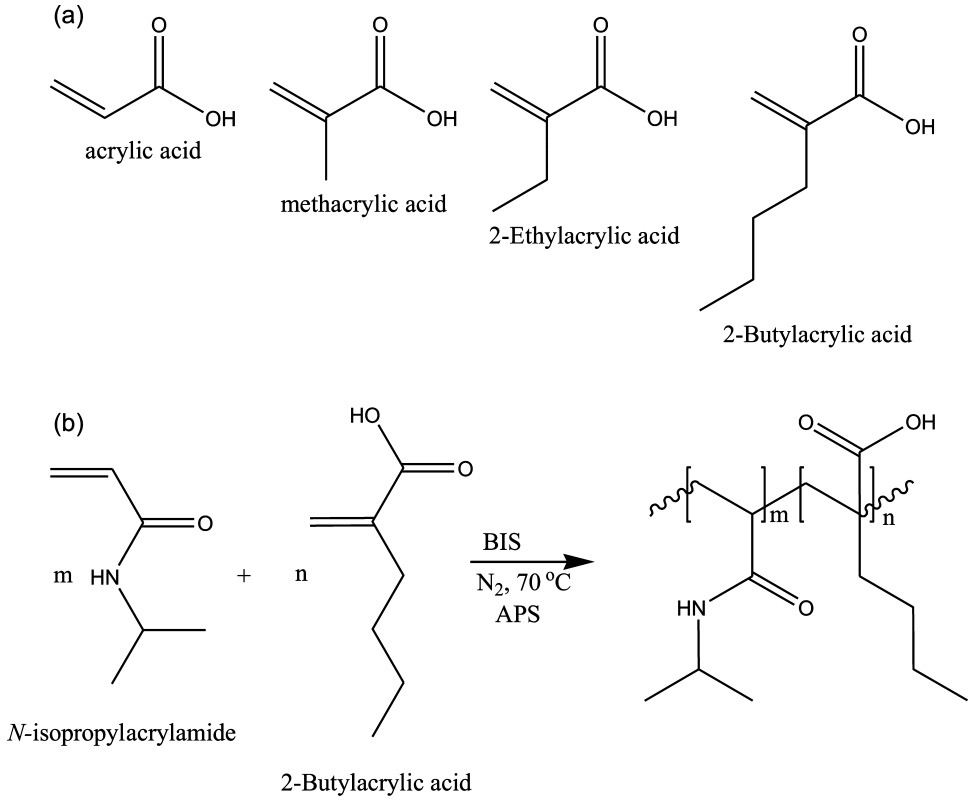

[a]A similar approach was used to generate all microgels used in this investigation.

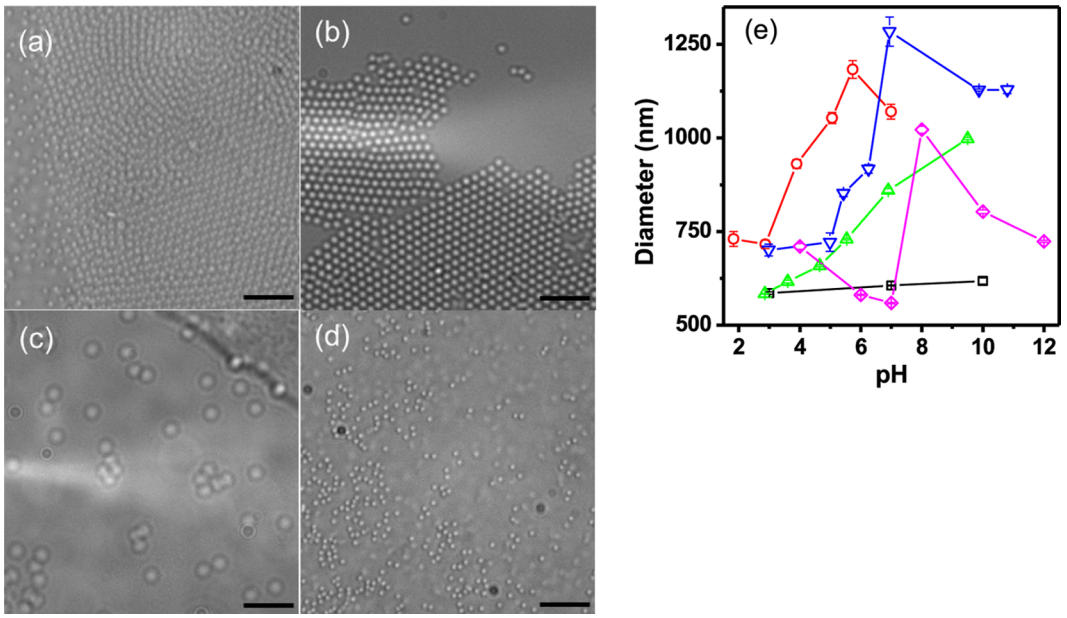

Figure 2. DIC images of (a) pNIPAm-*co*-AAc, (b) pNIPAm-*co*-MAAc, (c) pNIPAm-*co*-EAAc, (d) and pNIPAm-*co*-BAAc microgels, scale bar is 6 μm in each image. (e) DLS measured diameter of (□) pure pNIPAm microgel, (○) pNIPAm-*co*-AAc microgel, (▽) pNIPAm-*co*-MAAc microgel, (△) pNIPAm-*co*-EAAc microgel, and (◊) pNIPAm-*co*-BAAc microgel.

be much faster for the BAAc microgel-based devices compared to those of the others. Specifically, the BAAc microgel-based devices respond to pH changes within 2 s, whereas the others respond in 30 min (AAc), 3.5 min (MAAc), and 6.5 s (EAAc). The fast response of the BAAc microgel-based devices could be a result of the relatively long pendant alkyl group of the BAAc and its increased hydrophobicity. This creates a larger interstitial space between the chains, which increases chain mobility and yields faster shrinking/swelling kinetics.[44,45] This fast response can be used for various potential applications, for

DOI: 10.1021/acsomega.7b00103
ACS Omega 2017, 2, 1769−1777

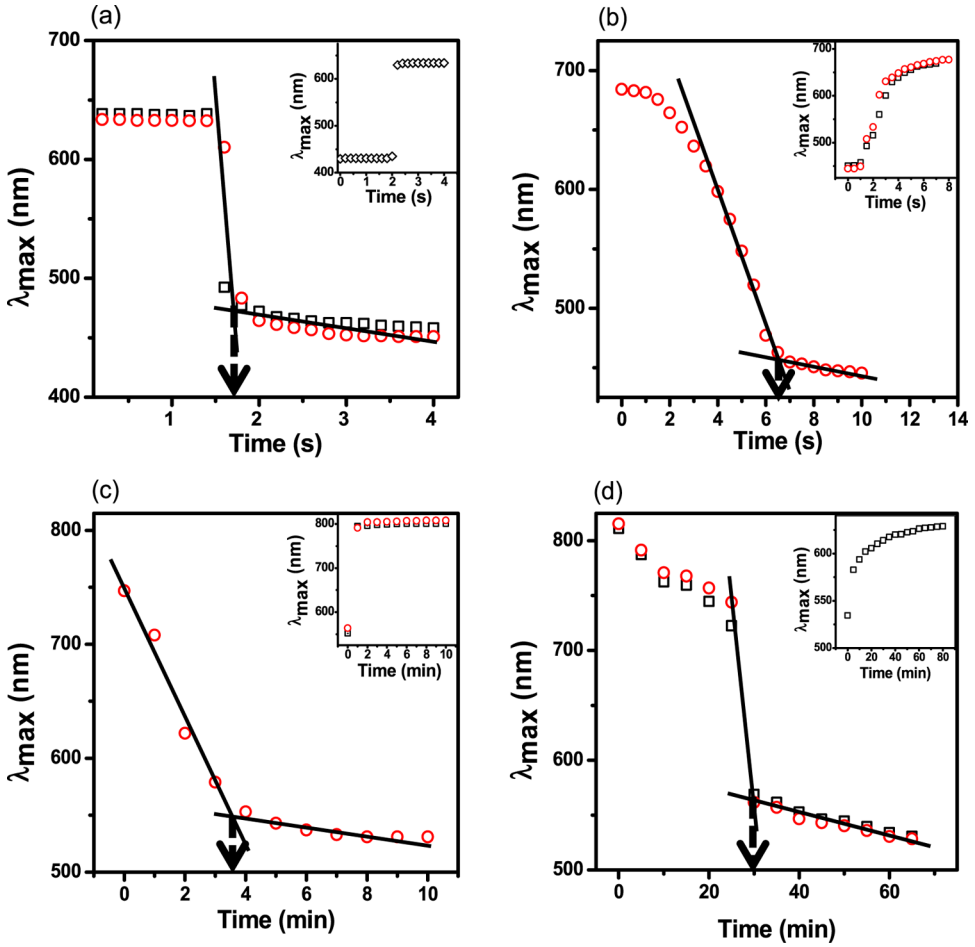

Figure 3. Kinetics of the response of (a) pNIPAm-*co*-BAAc, (b) pNIPAm-*co*-EAAc, (c) pNIPAm-*co*-MAAc, and (d) pNIPAm-*co*-AAc etalons to solution pH changes. The main figure in each case depicts the response kinetics going from high pH (10) to low pH (4 for (a); 3 for (b–d)). The insets represent the reverse, from low pH to high pH. In all cases, the solution pH was adjusted by addition of 1 M HCl or NaOH. The different data symbols represent data from different devices, and the arrows point to the critical time that the devices completed their response to pH.

example, the fabrication of rapid smart sensors and actuators, and rapid drug delivery systems.

RESULTS AND DISCUSSION

pH-responsive pNIPAm-based microgels were generated from the respective pH-responsive monomers (structures shown in Scheme 1a) using free radical precipitation polymerization at the conditions detailed in Scheme 1b. We point out that BAAc was synthesized following the synthetic route shown in Scheme S1, which yielded clear oil. Figure 2a–d shows the DIC microscopy images of the synthesized pNIPAm-based microgels. The resultant microgels were spherical with homogeneously distributed sizes without observable aggregates present. DLS was also used to determine the microgel diameter and the change in diameter as a result of solution pH changes. We expected to observe an increase in microgel diameter at pH > pK_a of the corresponding comonomers due to acid ionization and further, we expect the diameter to decrease at pH < pK_a due to subsequent acid neutralization. As can be seen in Figures 2e and S3, PNIPAm-based microgels are not responsive to pH changes, however microgels composed of AAc, MAAc, EAAc, and BAAc exhibit the expected pH response. That is, the pH-responsive microgels exhibit an increase in diameter at pH > pK_a, and return to their initial diameter at pH < pK_a. The observed decrease in average diameter between pH 4–6 and above pH 8 for BAAc, above 6 for AAc, and above 7 for EAAc could purely be an artifact of the DLS instrument, although we are not certain of the source.

Next, we constructed etalons from the microgels synthesized above. This was done by painting the microgels on a Au-coated glass substrate followed by the deposition of another Au layer on top of the formed microgel layer. This process has been described in the Experimental Section and in numerous previous publications.[48] As can be predicted from eq 1, an increase in *d*-spacing as a result of the deprotonation of the COOH groups (into COO^-) leads to an increase in the wavelength of light reflected from the device (i.e., a red shift). Multiple reflected wavelengths are expected from the devices as a result of the various orders of reflection (*m* in eq 1), which can be seen in Figure 1b. Hence, pH responses and response kinetics can be determined and compared by monitoring the position of a reflected peak of a given order as a function of time. To evaluate the responses of the devices to changes in solution pH, each device was immersed in an aqueous solution with a pH far above the pK_a of the acid comonomers, and the pH instantaneously decreased to well below the pK_a by fast addition of acid at a stir rate that was constant between experiments. The response kinetics for the devices to transition from a fully swollen to a fully collapsed state and vice-versa are shown in Figure 3. For applications such as smart actuators for

DOI: 10.1021/acsomega.7b00103
ACS Omega 2017, 2, 1769–1777

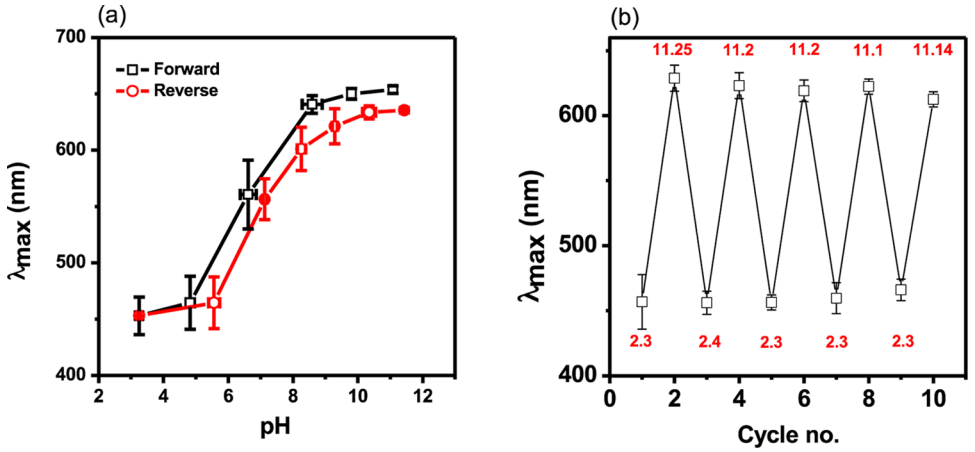

Figure 4. (a) Shifts in the reflectance peak position as a function of pH for the pNIPAm-*co*-BAAc etalons: (□) increasing pH and (○) decreasing pH. (b) The repeatability of the pNIPAm-*co*-BAAc etalon's response to solution pH. Each data point is the average obtained from three separate etalons with the error bars showing the standard deviation.

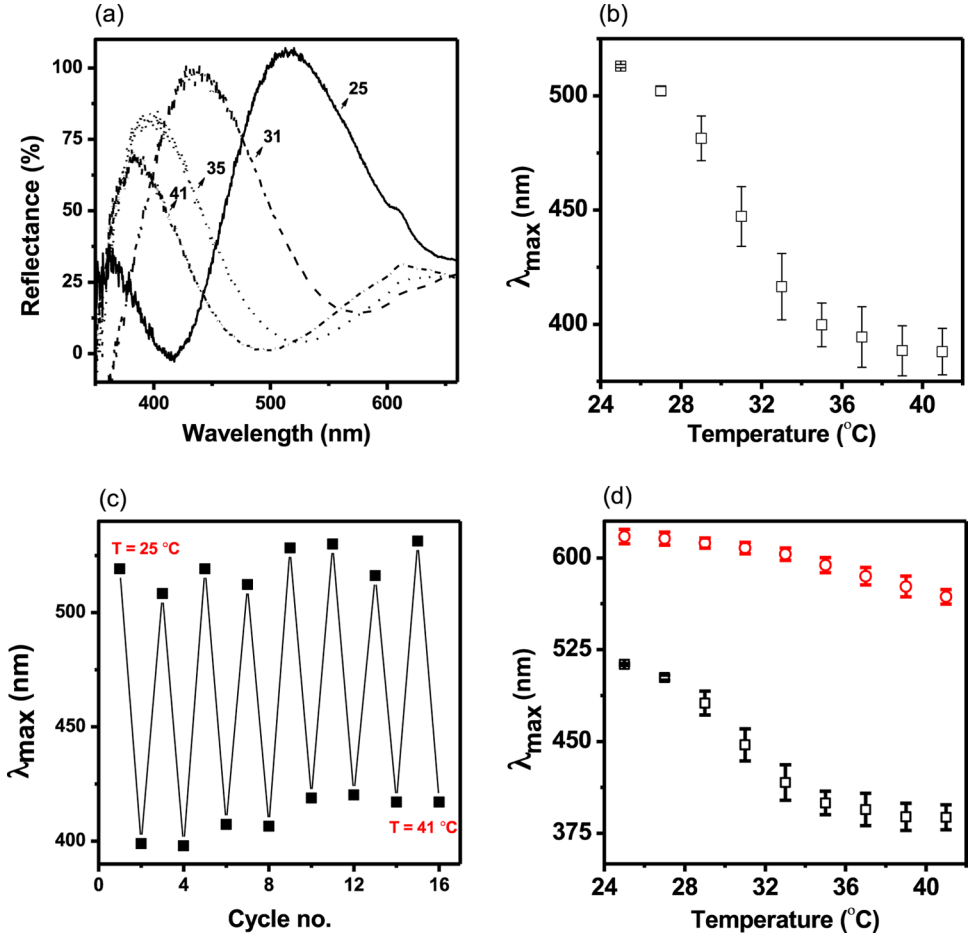

Figure 5. (a) Reflectance spectra from pNIPAm-*co*-BAAc etalons at the indicated temperatures at pH 3. (b) Peak position as a function of temperature. Data points in (b) are average of three devices and error bars represent the standard deviation. (c) Temperature cycling of pNIPAm-*co*-BAAc etalons between 25 and 41 °C at pH 3. (d) Temperature response of a pNIPAm-*co*-BAAc etalon at (○) pH 10 and (□) pH 3, well above and below the pK_a of BAAc, respectively.

chemical valves,[34] and on/off switches for chemical reactions,[36] a large-magnitude instantaneous response to the applied stimulus is desired. Impressively, it took less than 2 s for the pNIPAm-*co*-BAAc device to transition from a fully swollen state to a fully collapsed state. In comparison, pNIPAm-*co*-EAAc, pNIPAm-*co*-MAAc, and pNIPAm-*co*-AAc took relatively longer times; about 6.5 s, 3.5 min, and 30 min, respectively. Movies showing the fast response of pNIPAm-*co*-BAAc in comparison to that of pNIPAm-*co*-EAAc are shown in the ESI. It must be pointed out that all four microgels differ structurally due to the different lengths of the pendant alkyl groups on the AAc backbone (Scheme 1a). Hence, any difference in response can

DOI: 10.1021/acsomega.7b00103
ACS Omega 2017, 2, 1769−1777

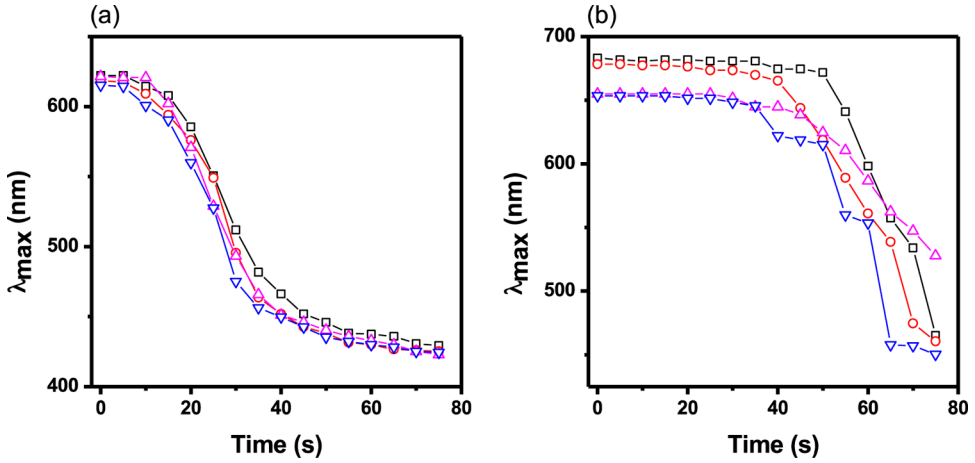

Figure 6. Temperature response kinetics for (a) pNIPAm-*co*-BAAc and (b) pNIPAm-*co*-AAc etalons. The temperature was set to increase from ∼23 to 60 °C at a heating rate of 0.6 °C s^{-1}. A single device was used in each case, and the data obtained as a function of the (□) first, (O) second, (△) third, and (▽) fourth heating cycle.

primarily be attributed to the pendant group chain length. We hypothesize that the "packing density" for a given "mass" of the microgels is higher for pNIPAm-*co*-AAc (due to the relatively smaller size of the AAc group) relative to that of the pNIPAm-*co*-BAAc microgels, which we predict will have a less dense internal structure due to the larger BAAc. The implication of this hypothesis is that the diffusion rate of water in and out of the microgels increases with increasing chain length of the pendant group of the microgels. This also permits rapid ionization and neutralization of the corresponding acid groups in the microgels.

We further explored the possibility of using the pNIPAm-*co*-BAAc etalon as a fast responding pH and temperature sensor. The pH range at which the device has the greatest response (highest sensitivity) was examined by immersing the device in a solution of low pH and gradually increasing the pH by addition of 0.1 M NaOH whilst monitoring the peak position. As can be seen from Figure 4a, the device responds to pH over the range of pH 6−9 and hence it can be used over the physiologically relevant pH range. We observed that the wavelength (λ_{max}) increased gradually below pH 6 (protonated form COOH) and sharply between 6 and 9 (deprotonated form COO^-), and plateaued beyond pH 9 (fully deprotonated) (Figure 4a). The reversibility of the device's response to pH was also probed as the pH was decreased by the addition of 0.1 M HCl. A phenomenon similar to the above has been observed in copolymers composed of AAc,[3,12,48,49] MAAc,[50] and propylacrylic acid (PAAc)[51] with NIPAm (pNIPAm-*co*-AAc, pNIPAm-*co*-MAAc, and pNIPAm-*co*-PAAc, respectively). We also investigated the device's response to repeated solution pH changes. This was done by immersing a single device in a solution of pH 2, allowing it to stabilize, and recording the spectrum. After stabilization, the pH was increased instantaneously to 11 by addition of 1.0 M NaOH, and again allowed to stabilize and a spectrum recorded. This process was repeated multiple times. As can be seen in Figure 4b, the device's response to repeated solution pH changes was highly reproducible, with a low standard deviation for the magnitude of the responses between devices. The ability to reuse a single device many times and still maintaining its performance is practically ideal from an economic point of view. Again, for the device to still maintain its performance between these extreme pH ranges suggests that the device can survive harsh pH conditions.

As pNIPAm is a well-known thermo-responsive polymer, we expected that copolymers composed of NIPAm should maintain their thermoresponsivity.[10] As shown in Figure 5 (and in Figures S3 and S4), the pNIPAm microgel-based devices maintained their thermoresponsivity. Specifically, as can be seen in Figure 5a, increasing solution temperature from 25 to 41 °C at pH 3 led to the expected blue shift of the peaks in the reflectance spectrum. The blue shift is a result of the decreased spacing between the two gold mirrors due to the collapse of the microgels. In Figure 5a, we have also shown the spectra for 25, 31, 35, and 41 °C for clarity. Figure 5b shows how the position of the reflectance peak depends on temperature. The wavelength decreased gradually as the temperature increased from 25 °C and then decreased sharply near the transition temperature of ∼31 °C. Above the transition temperature, the microgels are in their collapsed state; hence, no further decrease in wavelength was observed as the temperature was further increased above the primary transition temperature. Upon decreasing the solution temperature, the devices returned to their initial state, and the process can be repeated multiple times as can be seen in Figure 5c. We point out that the abrupt thermoresponsivity is observed at pH where the pNIPAm-*co*-BAAc microgels are in the protonated state (pH 3). At this pH, the microgels have no charge and can freely collapse and swell as the temperature is increased/decreased, respectively.[52] On the contrary, at higher pH > pK_a of BAAc, the pNIPAm-*co*-BAAc microgels are negatively charged and are swollen due to Coulombic repulsion of like charges and osmotic pressure build up within the microgel.[27] Therefore, any further attempt to change the microgel's diameter with temperature does not yield any significant transition, as the Coulombic force of repulsion[53] is greater than the entropy-driven collapse of the microgels. This is shown in Figure 5d for the pNIPAm-*co*-BAAc etalon device and in the Supporting Information for all of the microgels investigated here.

We also investigated the response kinetics of the pNIPAm-*co*-BAAc and pNIPAm-*co*-AAc microgel-based etalons to temperature. Here, the temperature control system was set to increase the solution temperature from ∼23 to 60 °C at a heating rate of 0.6 °C s^{-1}. The full response curves for both the pNIPAm-*co*-BAAc and pNIPAm-*co*-AAc microgel-based etalons

DOI: 10.1021/acsomega.7b00103
ACS Omega 2017, 2, 1769−1777

to this increased solution temperature are shown in Figure 6. We point out that a single device was used for multiple heating cycles and each curve in Figure 6 represents one heating cycle. As can be seen in Figure 6a, a rapid transition from the swollen to collapsed state (i.e., a blue shift in reflectance peak position) was observed for the pNIPAm-*co*-BAAc etalon, whereas the pNIPAm-*co*-AAc etalon (Figure 6b) exhibited much slower response kinetics at the same heating rate and solution pH. This observation further supports our hypothesis above that the hydrophobic effect (with increased void space) can lead to an increased diffusion rate of water in and out of the microgels with increased chain length of the pendant group (BAAc). These points taken together lead to the enhanced response kinetics.

CONCLUSIONS

We have synthesized pH-responsive microgels that exhibit responses over a broad pH range. Furthermore, we have generated optical devices composed of the microgels that exhibit optical properties that depend on solution pH. As a result of these studies, we found that some of the devices exhibited unusually fast response kinetics that we found to depend on the length of the pendant group on the acid incorporated in the microgels. Specifically, the response to pH was the fastest for the pNIPAm-*co*-BAAc etalon, whereas the pNIPAm-*co*-AAc etalon exhibited the slowest response. We hypothesized that this enhanced response speed can be attributed to: (1) the increased hydrophobicity of the pNIPAm-*co*-BAAc microgel, which can lead to a faster transition to its deswollen state; and/or (2) the length of the butyl group on BAAc creating a lower packing density and a less dense internal structure, resulting in a larger interstitial space between chains and increased chain mobility and faster shrinking/swelling kinetics. These hypotheses were further supported by an investigation of the temperature response kinetics, which were improved for the pNIPAm-*co*-BAAc etalon relative to those of the pNIPAm-*co*-AAc etalon. With this knowledge, low cost and easy to use pH (and related) sensors could be developed for a wide variety of applications where rapid response time is of great importance.

EXPERIMENTAL SECTION

Materials. Unless otherwise specified, all reagents were purchased from Sigma-Aldrich (Oakville, ON, Canada). NIPAm was purified by re-crystallization from hexanes and vacuum dried. *N*,*N*′-methylene(bisacrylamide) (BIS), ammonium persulfate (APS), AAc, MAAc, EAAc, piperidine, formaldehyde, ethanol, *n*-butylmalonic acid, ethyl acetate, and anhydrous $MgSO_4$ were used without further purification. 2-BAAc was synthesized following the procedure reported by Pratt et al.[46] with some modifications. A pH meter (JENCO 6173 pH, San Diego, CA) was used to prepare solutions with known pH, using sodium hydroxide (NaOH) and hydrochloric acid (HCl) to adjust the pH. A conductivity meter (Orion Star A212, Indonesia) was used for conductivity measurements. Millipore water (18.2 MΩ cm) from a Milli-Q Plus system (Z00QSVC01; Fisher, Toronto, ON, Canada) was used for all experiments. A Rotovap RV 8 (IKA, Wilmington, NC) was used to remove organic solvents.

Synthesis of BAAc. BAAc was synthesized using a modified version of what was reported by Pratt et al.[46] Specifically, piperidine (7.5 mmol, 0.74 mL) and formaldehyde (31.3 mmol, 2.3 mL) were added to a solution of *n*-butylmalonic acid (6.2, mmol, 1.00 g) in ethanol (11.6 mL). The solution was heated to 85 °C under reflux with stirring, during which a white precipitate appeared and steadily re-dissolved over 1 h. The mixture was stirred at 85 °C (under reflux) overnight and then cooled to room temperature. The solvent was removed under reduced pressure using rotoevaporation. The residue was then dissolved in ethyl acetate (12 mL) and transferred into a separatory funnel. The mixture was washed successively with 1.0 M HCl and brine (5%), dried over anhydrous $MgSO_4$, and vacuum-filtered (Whatman #1 filter paper) yielding a clear oil. ^{1}H NMR ($CDCl_3$, 500 MHz): δ_H 6.27 (s, 1H), 5.63 (s, 1H), 2.32−2.28 (m, 2H), 1.49−1.23 (m, 4H), 0.91 (t, 3H). Mass spectrometry (MS) was also used to characterize the BAAc, and revealed the molecular ion peak of (M − H) at 127.0764, see Supporting Information. Fourier transform infrared (FTIR) spectra of both BAAc and pNIPAm-*co*-BAAc are also shown in the Supporting Information, and exhibit the expected vibrational frequencies at 2960 cm^{-1} (O−H), 2875 cm^{-1} (═CH), 1697 cm^{-1} (C═O), and 1629 cm^{-1} (C═C).

Synthesis of pNIPAm-Based Microgels. The microgels were synthesized by free radical precipitation polymerization, similar to a previously published procedure.[47,48] NIPAm (11.928 mmol) and BIS (0.702 mmol) were weighed into a 250 mL beaker with 99 mL of deionized (DI) water. The mixture was stirred for 0.5 h and filtered through a 0.2 μm filter into a 3-necked round bottom flask. A reflux condenser was added to the flask, along with a N_2 gas inlet (needle) and temperature probe. The solution was bubbled with N_2 gas and allowed to heat to 70 °C over 1.5 h. One of the acids, for example, BAAc/EAAc/MAAc/AAc (1.403 mmol), was added to the heated reaction mixture in one aliquot, and the polymerization was immediately initiated by the addition of APS (0.2 mmol) dissolved in 1 mL of DI water. The solution turned white/cloudy after ∼1 min, showing successful initiation. The reaction was then allowed to proceed at 70 °C for 4 h under a blanket of N_2 gas. The resulting suspension was allowed to cool overnight, followed by filtration through glass wool to remove any large aggregates. The microgel solution was then distributed into centrifuge tubes and purified via centrifugation at ∼10 000 rpm for ∼30 min to form a pellet, followed by removal of the supernatant and resuspension in DI water; this was repeated 6×. The purified microgels were stored for further use. The actual amount of ionic comonomers in the microgels was estimated by potentiometric and conductometric titrations, as shown in the Supporting Information.

Preparation of Etalons. Etalons were fabricated according to our group's previously published "paint on" protocol.[43] Briefly, Au-coated coverslips (etalon underlayer) were fabricated by depositing 2 nm of Cr and 15 nm of Au onto a 25 × 25 mm^2 ethanol-rinsed and N_2 gas-dried glass coverslip (Fisher's Finest, Ottawa, ON) via thermal evaporation at a rate of 1 and 0.1 Å s^{-1}, respectively (Torr International Inc., thermal evaporation system, model THEUPG, New Windsor, NY). The Cr/Au substrates were annealed at 250 °C for 3 h (Thermolyne muffle furnace, Ottawa, ON, Canada) and cooled to room temperature prior to microgel film deposition. The annealed glass slides were rinsed with ethanol and water followed by N_2 gas drying. The concentrated microgel pellets obtained via centrifugation were vortexed to loosen and homogenize the microgels, and a 40 μL aliquot of concentrated microgel was spread onto the annealed 25 mm × 25 mm Au-coated glass coverslip. The film was allowed to dry on a 30 °C hotplate for 2

DOI: 10.1021/acsomega.7b00103
ACS Omega 2017, 2, 1769−1777

h followed by rinsing of the excess microgels with DI water. The samples were soaked overnight at 30 °C in a DI water bath. The samples were then rinsed with DI water, dried with N_2, and another Au overlayer (2 nm Cr for adhesion, followed by 15 nm Au) was deposited under the same conditions as the underlayer. The completed device was soaked in DI water overnight at 30 °C, after which the etalon assembly (Figure 1a) was ready for spectral analysis.

Characterization. DIC microscope images were acquired on an Olympus inverted research microscope (IX71), at 100× magnification. Hydrodynamic diameters were measured on a Malvern Instruments (Westborough, MA) Zetasizer Nano ZS equipped with a 633 nm laser. NMR spectra were collected using an Agilent/Varian Inova four-channel 500 MHz spectrometer (Santa Clara, CA), with $CDCl_3$ as solvent. Reflectance measurements for the etalons in response to solution pH and temperature were obtained using a Red Tide USB650 spectrometer, a LS-1 tungsten light source, and a reflectance probe from Ocean Optics (Dunedin, FL). The spectra were recorded using Ocean Optics Spectra Suite Spectroscopy Software over a wavelength range of 350−1000 nm. A custom-built temperature controlled chamber (Electronic Department, University of Alberta) was used to maintain solution temperature and hold the etalon in a stable position. We point out that a 0.6 °C change in temperature was observed as a result of the neutralization reaction required to change the solution pH. Despite this, this temperature change is not significant enough to contribute to the observed kinetics. Additionally, the experimental conditions for all of the devices were constant, and therefore the temperature effect can be ignored, and the response kinetics to solution pH changes can be directly compared. Videos were recorded using a Samsung Galaxy S6 edge, 16 MP OIS (F1.9). Infrared spectra were collected on a Thermo Nicolet 8700 FTIR Spectrometer, and MS was run on an orthogonal acceleration TOF6220 ESI in negative ion mode (Agilent Technologies, Santa Clara, CA) operating in full scan mode.

■ ASSOCIATED CONTENT

Supporting Information

The Supporting Information is available free of charge on the ACS Publications website at DOI: 10.1021/acsomega.7b00103.

Mass spectrum of BAAc, FTIR of BAAc, pNIPAm-*co*-AAc, pNIPAm-*co*-MAAc, pNIPAm-*co*-EAAc, and pNIPAm-*co*-BAAc (PDF)

Movies showing pH response kinetics for pNIPAm-*co*-EAAc and pNIPAm-*co*-BAAc; potentiometric and conductometric titrations; LCST measurement for pNIPAm, pNIPAm-*co*-AAc, pNIPAm-*co*-MAAc, pNIPAm-*co*-EAAc, and pNIPAm-*co*-BAAc (MPG) (MPG)

■ AUTHOR INFORMATION

Corresponding Author

*E-mail: michael.serpe@ualberta.ca.

ORCID

Michael J. Serpe: 0000-0002-0161-1087

Notes

The authors declare no competing financial interest.

■ ACKNOWLEDGMENTS

M.J.S. acknowledges funding from the University of Alberta (the Department of Chemistry and the Faculty of Science), the Natural Sciences and Engineering Research Council of Canada (NSERC), the Canada Foundation for Innovation (CFI), the Alberta Advanced Education & Technology Small Equipment Grants Program (AET/SEGP), Grand Challenges Canada and IC-IMPACTS.

■ REFERENCES

(1) Dalmont, H.; Pinprayoon, O.; Saunders, B. R. Study of pH-responsive microgels containing methacrylic acid: Effects of particle composition and added calcium. *Langmuir* **2008**, *24*, 2834−2840.

(2) Hu, L.; Serpe, M. J. Controlling the response of color tunable poly(N-isopropylacrylamide) microgel-based etalons with hysteresis. *Chem. Commun.* **2013**, *49*, 2649−2651.

(3) Johnson, K. C.; Mendez, F.; Serpe, M. J. Detecting solution pH changes using poly (N-isopropylacrylamide)-co-acrylic acid microgel-based etalon modified quartz crystal microbalances. *Anal. Chim. Acta* **2012**, *739*, 83−88.

(4) Gao, Y.; Ahiabu, A.; Serpe, M. J. Controlled drug release from the aggregation-disaggregation behavior of pH-responsive microgels. *ACS Appl. Mater. Interfaces* **2014**, *6*, 13749−13756.

(5) Schmaljohann, D. Thermo- and pH-responsive polymers in drug delivery. *Adv. Drug Delivery Rev.* **2006**, *58*, 1655−1670.

(6) Jochum, F. D.; Theato, P. Temperature- and light-responsive smart polymer materials. *Chem. Soc. Rev.* **2013**, *42*, 7468−7483.

(7) Yuk, S. H.; Cho, S. H.; Lee, S. H. pH/temperature-responsive polymer composed of poly((N,N-dimethylamino)ethyl methacrylate-co-ethylacrylamide). *Macromolecules* **1997**, *30*, 6856−6859.

(8) Stuart, M. A. C.; Huck, W. T. S.; Genzer, J.; Mueller, M.; Ober, C.; Stamm, M.; Sukhorukov, G. B.; Szleifer, I.; Tsukruk, V. V.; Urban, M.; Winnik, F.; Zauscher, S.; Luzinov, I.; Minko, S. Emerging applications of stimuli-responsive polymer materials. *Nat. Mater.* **2010**, *9*, 101−113.

(9) Dai, S.; Ravi, P.; Tam, K. C. Thermo- and photo-responsive polymeric systems. *Soft Matter* **2009**, *5*, 2513−2533.

(10) Lyon, L. A.; Meng, Z.; Singh, N.; Sorrell, C. D.; John, A. S. Thermoresponsive microgel-based materials. *Chem. Soc. Rev.* **2009**, *38*, 865−874.

(11) Zhou, J.; Wang, G.; Hu, J.; Lu, X.; Li, J. Temperature, ionic strength and pH induced electrochemical switching of smart polymer interfaces. *Chem. Commun.* **2006**, 4820−4822.

(12) Shibayama, M.; Ikkai, F.; Inamoto, S.; Nomura, S.; Han, C. C. pH and salt concentration dependence of the microstructure of poly (N-isopropylacrylamide-co-acrylic acid) gels. *J. Chem. Phys.* **1996**, *105*, 4358−4366.

(13) Xu, W.; Gao, Y.; Serpe, M. J. Electrochemically color tunable poly (N-isopropylacrylamide) microgel-based etalons. *J. Mater. Chem. C* **2014**, *2*, 3873−3878.

(14) Thévenot, J.; Oliveira, H.; Sandre, O.; Lecommandoux, S. Magnetic responsive polymer composite materials. *Chem. Soc. Rev.* **2013**, *42*, 7099−7116.

(15) Zhang, Q. M.; Xu, W.; Serpe, M. J. Optical devices constructed from multiresponsive microgels. *Angew. Chem., Int. Ed.* **2014**, *53*, 4827−4831.

(16) Heskins, M.; Guillet, J. E. Solution properties of poly (N-isopropylacrylamide). *J. Macromol. Sci., Part A: Chem.* **1968**, *2*, 1441−1455.

(17) Islam, M. R.; Serpe, M. J. Polymer-based devices for the label-free detection of DNA in solution: low DNA concentrations yield large signals. *Anal. Bioanal. Chem.* **2014**, *406*, 4777−4783.

(18) Hendrickson, G. R.; Lyon, L. A. Bioresponsive hydrogels for sensing applications. *Soft Matter* **2009**, *5*, 29−35.

(19) Gao, Y.; Zago, G. P.; Jia, Z.; Serpe, M. J. Controlled and triggered small molecule release from a confined polymer film. *ACS Appl. Mater. Interfaces* **2013**, *5*, 9803−9808.

DOI: 10.1021/acsomega.7b00103
ACS Omega 2017, 2, 1769−1777

(20) Gao, Y.; Ahiabu, A.; Serpe, M. J. Controlled drug release from the aggregation−disaggregation behavior of pH-responsive microgels. *ACS Appl. Mater. Interfaces* **2014**, *6*, 13749−13756.
(21) Mura, S.; Nicolas, J.; Couvreur, P. Stimuli-responsive nanocarriers for drug delivery. *Nat. Mater.* **2013**, *12*, 991−1003.
(22) Lee, K. Y.; Mooney, D. J. Hydrogels for tissue engineering. *Chem. Rev.* **2001**, *101*, 1869−1879.
(23) Zhai, L. Stimuli-responsive polymer films. *Chem. Soc. Rev.* **2013**, *42*, 7148−7160.
(24) Ahn, S.-k.; Kasi, R. M.; Kim, S.-C.; Sharma, N.; Zhou, Y. Stimuli-responsive polymer gels. *Soft Matter* **2008**, *4*, 1151−1157.
(25) Guan, Y.; Zhang, Y. PNIPAM microgels for biomedical applications: from dispersed particles to 3D assemblies. *Soft Matter* **2011**, *7*, 6375−6384.
(26) Thorne, J. B.; Vine, G. J.; Snowden, M. J. Microgel applications and commercial considerations. *Colloid Polym. Sci.* **2011**, *289*, 625−646.
(27) Schroeder, R.; Rudov, A. A.; Lyon, L. A.; Richtering, W.; Pich, A.; Potemkin, I. I. Electrostatic Interactions and Osmotic Pressure of Counterions Control the pH-Dependent Swelling and Collapse of Polyampholyte Microgels with Random Distribution of Ionizable Groups. *Macromolecules* **2015**, *48*, 5914−5927.
(28) Dai, S.; Ravi, P.; Tam, K. C. pH-Responsive polymers: synthesis, properties and applications. *Soft Matter* **2008**, *4*, 435−449.
(29) Hoare, T.; Pelton, R. Highly pH and Temperature Responsive Microgels Functionalized with Vinylacetic Acid. *Macromolecules* **2004**, *37*, 2544−2550.
(30) Brugger, B.; Richtering, W. Emulsions Stabilized by Stimuli-Sensitive Poly(N-isopropylacrylamide)-co-Methacrylic Acid Polymers: Microgels versus Low Molecular Weight Polymers. *Langmuir* **2008**, *24*, 7769−7777.
(31) Yin, X. C.; Stover, H. D. H. Thermosensitive and pH-sensitive polymers based on maleic anhydride copolymers. *Macromolecules* **2002**, *35*, 10178−10181.
(32) Wang, B.; Xu, X.-D.; Wang, Z.-C.; Cheng, S.-X.; Zhang, X.-Z.; Zhu, R.-X. Synthesis and properties of pH and temperature sensitive P(NIPAAm-co-DMAEMA) hydrogels. *Colloids Surf., B* **2008**, *64*, 34−41.
(33) Grainger, S. J.; El-Sayed, M. E. Stimuli-Sensitive Particles for Drug Delivery. In *Biologically-Responsive Hybrid Biomaterials*; World Scientific Publishing Co. Pte. Ltd, 2010; pp 171−189.
(34) Beebe, D. J.; Moore, J. S.; Bauer, J. M.; Yu, Q.; Liu, R. H.; Devadoss, C.; Jo, B. H. Functional hydrogel structures for autonomous flow control inside microfluidic channels. *Nature* **2000**, *404*, 588−590.
(35) Takashima, Y.; Hatanaka, S.; Otsubo, M.; Nakahata, M.; Kakuta, T.; Hashidzume, A.; Yamaguchi, H.; Harada, A. Expansion-contraction of photoresponsive artificial muscle regulated by host-guest interactions. *Nat. Commun.* **2012**, *3*, No. 1270.
(36) Kumacheva, E. Hydrogels: The catalytic curtsey. *Nat. Mater.* **2012**, *11*, 665−666.
(37) Zhang, J.; Xie, R.; Zhang, S.-B.; Cheng, C.-J.; Ju, X.-J.; Chu, L.-Y. Rapid pH/temperature-responsive cationic hydrogels with dual stimuli-sensitive grafted side chains. *Polymer* **2009**, *50*, 2516−2525.
(38) Yan, H.; Fujiwara, H.; Sasaki, K.; Tsujii, K. Rapid swelling/collapsing behavior of thermoresponsive poly(N-isopropylacrylamide)gel containing poly(2-(methacryloyloxy)-decylphosphate) surfactant. *Angew. Chem., Int. Ed.* **2005**, *44*, 1951−1954.
(39) Musch, J.; Schneider, S.; Lindner, P.; Richtering, W. Unperturbed volume transition of thermosensitive poly-(N-isopropylacrylamide) microgel particles embedded in a hydrogel matrix. *J. Phys. Chem. B* **2008**, *112*, 6309−6314.
(40) Yoshida, R.; Uchida, K.; Kaneko, Y.; Sakai, K.; Kikuchi, A.; Sakurai, Y.; Okano, T. Comb-type grafted hydrogels with rapid de-swelling response to temperature-changes. *Nature* **1995**, *374*, 240−242.
(41) Zhang, J.; Chu, L.-Y.; Li, Y.-K.; Lee, Y. M. Dual thermo- and pH-sensitive poly(N-isopropylacrylamide-co-acrylic acid) hydrogels with rapid response behaviors. *Polymer* **2007**, *48*, 1718−1728.
(42) Xia, L.-W.; Xie, R.; Ju, X.-J.; Wang, W.; Chen, Q.; Chu, L.-Y. Nano-structured smart hydrogels with rapid response and high elasticity. *Nat. Commun.* **2013**, *4*, No. 2226.
(43) Sorrell, C. D.; Carter, M. C. D.; Serpe, M. J. A "Paint-On" Protocol for the Facile Assembly of Uniform Microgel Coatings for Color Tunable Etalon Fabrication. *ACS Appl. Mater. Interfaces* **2011**, *3*, 1140−1147.
(44) Kaneko, Y.; Sakai, K.; Kikuchi, A.; Yoshida, R.; Sakurai, Y.; Okano, T. Influence of freely mobile grafted chain length on dynamic properties of comb-type grafted poly (N-isopropylacrylamide) hydrogels. *Macromolecules* **1995**, *28*, 7717−7723.
(45) Kaneko, Y.; Sakai, K.; Kikuchi, A.; Sakurai, Y.; Okano, T. Fast Swelling/Deswelling Kinetics of Comb-type Grafted Poly (N-isopropylacrylamide) Hydrogels. *Macromol. Symp.* **1996**, *109*, 41−43.
(46) Pratt, L. M.; Keavy, K. N.; Pain, G. D.; Mounier, L. Antibacterial Agents. U.S. Patent 6,846,825, Jan 25, 2005.
(47) Debord, J. D.; Lyon, L. A. Synthesis and characterization of pH-responsive copolymer microgels with tunable volume phase transition temperatures. *Langmuir* **2003**, *19*, 7662−7664.
(48) Sorrell, C. D.; Carter, M. C.; Serpe, M. J. Color Tunable Poly (N-Isopropylacrylamide)-co-Acrylic Acid Microgel−Au Hybrid Assemblies. *Adv. Funct. Mater.* **2011**, *21*, 425−433.
(49) Zhang, X.-Z.; Yang, Y.-Y.; Wang, F.-J.; Chung, T.-S. Thermosensitive Poly(N-isopropylacrylamide-co-acrylic acid) Hydrogels with Expanded Network Structures and Improved Oscillating Swelling−Deswelling Properties. *Langmuir* **2002**, *18*, 2013−2018.
(50) Hoare, T.; Pelton, R. Functional Group Distributions in Carboxylic Acid Containing Poly(N-isopropylacrylamide) Microgels. *Langmuir* **2004**, *20*, 2123−2133.
(51) Yin, X.; Hoffman, A. S.; Stayton, P. S. Poly(N-isopropylacrylamide-co-propylacrylic acid) Copolymers That Respond Sharply to Temperature and pH. *Biomacromolecules* **2006**, *7*, 1381−1385.
(52) Polotsky, A. A.; Plamper, F. A.; Borisov, O. V. Collapse-to-Swelling Transitions in pH- and Thermoresponsive Microgels in Aqueous Dispersions: The Thermodynamic Theory. *Macromolecules* **2013**, *46*, 8702−8709.
(53) Cho, J. K.; Meng, Z.; Lyon, L. A.; Breedveld, V. Tunable attractive and repulsive interactions between pH-responsive microgels. *Soft Matter* **2009**, *5*, 3599−3602.

DOI: 10.1021/acsomega.7b00103
ACS Omega 2017, 2, 1769−1777